



## Sorption and transport of aqueous Fe(II) in a goethite-coated sand column under anoxic conditions.

Khalil Hanna, Muhammad Usman, Vincent Chatain

### ► To cite this version:

Khalil Hanna, Muhammad Usman, Vincent Chatain. Sorption and transport of aqueous Fe(II) in a goethite-coated sand column under anoxic conditions.. Applied Geochemistry, 2013, 35, pp.255-263. 10.1016/j.apgeochem.2013.04.017 . hal-00914368

**HAL Id: hal-00914368**

**<https://hal-univ-rennes1.archives-ouvertes.fr/hal-00914368>**

Submitted on 11 Dec 2013

**HAL** is a multi-disciplinary open access archive for the deposit and dissemination of scientific research documents, whether they are published or not. The documents may come from teaching and research institutions in France or abroad, or from public or private research centers.

L'archive ouverte pluridisciplinaire **HAL**, est destinée au dépôt et à la diffusion de documents scientifiques de niveau recherche, publiés ou non, émanant des établissements d'enseignement et de recherche français ou étrangers, des laboratoires publics ou privés.

# **Sorption and transport of aqueous Fe<sup>II</sup> in a goethite-coated sand column under anoxic conditions**

K. Hanna <sup>a, b, c</sup> \*, M. Usman <sup>c, d</sup>, V. Chatain <sup>e</sup>

<sup>a</sup> Ecole Nationale Supérieure de Chimie de Rennes, UMR CNRS 6226, Avenue du Général Leclerc, 35708 Rennes Cedex 7, France.

<sup>b</sup> Université Européenne de Bretagne, France.

<sup>c</sup> Laboratoire de Chimie Physique et Microbiologie pour l'Environnement, LCPME, UMR 7564 CNRS-Université de Lorraine, 405 rue de Vandoeuvre, 54600, Villers Les Nancy, France.

<sup>d</sup> Institute of Soil and Environmental Sciences, University of Agriculture, Faisalabad, 38040, Pakistan.

<sup>e</sup> Université de Lyon, INSA-Lyon, Laboratoire de Génie Civil et d'Ingénierie Environnementale LGCIE, 20 avenue Albert Einstein, 69621 Villeurbanne, France.

*\* Corresponding author:*

Ecole Nationale Supérieure de Chimie de Rennes  
Avenue du Général Leclerc, 35708 Rennes Cedex 7, France.

Tel: 00 33 2 23 23 80 27

Fax: 00 33 2 23 23 81 20

[khalil.hanna@ensc-rennes.fr](mailto:khalil.hanna@ensc-rennes.fr)

## **Abstract**

Experiments were conducted under static batch and dynamic flow conditions to evaluate the sorption of  $\text{Fe}^{\text{II}}$  onto three goethites (G1, G2 and G3) having different crystal habits, morphologies and surface properties. Results reveal that G1 exhibited the highest  $\text{Fe}^{\text{II}}$  sorption extent and lowest kinetic rate constant, which may result from higher surface site density, surface roughness and edge surface faces. Surface complexation modeling parameters derived from batch experiments were combined with hydrodynamic parameters to simulate breakthrough curves in goethite-coated sand packed columns. The total sorbed amount of  $\text{Fe}^{\text{II}}$  at complete breakthrough was in agreement with that expected from the batch experiments, except for G1. Sorption breakthrough predictions that make use of surface complexation parameters accurately predicted  $\text{Fe}^{\text{II}}$  mobility in G2 and G3 columns, but poorly in G1 column. Experiments at various flow rates in G1 columns represented different amounts of  $\text{Fe}^{\text{II}}$  sorbed at complete breakthrough, thereby underscoring the impact of kinetic sorption. Moreover, Fe dissolution/re-precipitation or  $\text{Fe}^{\text{II}}$ -induced transformation of goethite was suspected at the lowest flow rate in the G1 column. The influence of goethite phase specific reactivity on  $\text{Fe}^{\text{II}}$  sorption under batch versus advective-dispersive flow is herein demonstrated. These findings have strong implications to assess transport of  $\text{Fe}^{\text{II}}$  and environmental contaminants both in natural and engineered systems.

**Keywords:** goethite;  $\text{Fe}^{\text{II}}$ ; sorption; transport; column; modeling.

## Introduction

In natural environments, the iron oxides exhibit considerable crystallographic heterogeneity, ranging from poorly crystalline phases such as 2-line ferrihydrite to well crystalline ones like goethite and hematite with different characteristics (Cornell and Schwertmann, 1996; Schwertmann and Cornell, 2000). Goethite ( $\alpha$ -FeOOH) is by far the most common iron oxide in soils and sediments due to its high thermodynamic stability (Cornell and Schwertmann, 1996; Schwertmann and Cornell, 2000). The morphology, crystallography and specific surface area of goethite can vary widely (Cornell and Schwertmann, 1996; Schwertmann and Cornell, 2000).

Dissolved  $\text{Fe}^{\text{II}}$  is formed as a result of many biotic and abiotic processes in natural systems (Stumm and Sulzberger, 1992). The interactions of  $\text{Fe}^{\text{II}}$  with environmental surfaces such as iron oxides have attracted a great deal of attention not only because of the complicated chemical processes such as sorption and mineralogical transformation, but also because the reaction has significant environmental implications (Coughlin and Stone, 1995; Liger et al., 1999; Hofstetter et al., 1999; Elsner et al., 2004; Williams and Scherer, 2004; Pedersen et al., 2005; Dixit and Hering, 2006; Larese-Casanova and Scherer, 2007; Tobler et al., 2007; Amstaetter et al., 2009; Handler et al., 2009; Usman et al., 2012a; Usman et al., 2012b). The studies of the interaction between  $\text{Fe}^{\text{II}}$  and mineral species focus on the catalytic effects of  $\text{Fe}^{\text{II}}$  for contaminants reduction and also on mineralogical transformation of  $\text{Fe}^{\text{III}}$ -oxyhydroxides. Aqueous  $\text{Fe}^{\text{II}}$  complexes can reduce a number of contaminants but sorbed  $\text{Fe}^{\text{II}}$  or structural  $\text{Fe}^{\text{II}}$  are often more powerful reductants than dissolved  $\text{Fe}^{\text{II}}$  (Hofstetter et al., 1999; Elsner et al., 2004; Tobler et al., 2007; Amstaetter et al., 2009). The interaction of aqueous  $\text{Fe}^{\text{II}}$  with iron oxides can produce a variety of reactions including sorption, electron transfer between  $\text{Fe}^{\text{II}}$  and  $\text{Fe}^{\text{III}}$ -oxide, conduction, dissolution, atom exchange and/or transformation to secondary minerals (Williams and Scherer, 2004; Pedersen et al., 2005; Larese-Casanova and Scherer, 2007; Handler et al., 2009).

Interfacial electron transfer reactions between sorbed  $\text{Fe}^{\text{II}}$  and well crystallized iron oxides (e.g. goethite, hematite) has been experimentally evidenced using Mössbauer spectroscopy (Williams and Scherer, 2004). Moreover, at low  $\text{Fe}^{\text{II}}$  dose, sorption of  $\text{Fe}^{\text{II}}$  on these iron oxides have been quantified and described through both macroscopic and surface complexation modeling approaches (Coughlin and Stone, 1995; Liger et al., 1999; Dixit and Hering, 2006; Hiemstra and van Riemsdijk, 2007). Both sorption extent and rate have also

been determined although sorbed  $\text{Fe}^{\text{II}}$  may transfer an electron to the solid matrix (Liger et al., 1999; Dixit and Hering, 2006; Hiemstra and van Riemsdijk, 2007).

The effect of crystal structure and morphology on  $\text{Fe}^{\text{II}}$  sorption is not yet fully evaluated that will be done in this study by involving three kinds of same iron oxide (i.e. goethite). Large variability of goethite exists in both natural and engineering systems but no study has been reported comparing sorption of  $\text{Fe}^{\text{II}}$  onto different goethites. While the interactions of  $\text{Fe}^{\text{II}}$  with Fe-oxides are widely studied in laboratory batch reactors (Coughlin and Stone, 1995; Williams and Scherer, 2004; Pedersen et al., 2005; Dixit and Hering, 2006; Hiemstra and van Riemsdijk, 2007; Larese-Casanova and Scherer, 2007; Handler et al., 2009; Usman et al., 2013), reports on transport of  $\text{Fe}^{\text{II}}$  in goethite-packed column under anoxic flow through conditions are still missing in literature. In contrast to batch studies, continuous flow experiments allow studying the impact of non-equilibrium sorption on transport and impact of hydrodynamic parameters such as dispersion on the breakthrough of solute. Column tests can also accommodate more accurate field estimation by providing an appropriate soil/aqueous phase ratio. In addition, the byproducts of redox reaction are flushed out in continuous flow experiments, which can modify the kinetics and extent of reaction.

In the present study, the sorption extent of  $\text{Fe}^{\text{II}}$  onto three kinds of goethite (G1, G2 and G3) having different crystal habits, morphologies and surface properties was compared. Sorption of  $\text{Fe}^{\text{II}}$  was evaluated *vs.* time and pH in batch experiments. In order to evaluate the implication of non-equilibrium/kinetics processes in the breakthrough behavior, flow through experiments were conducted at different flow rates and column residence times. Predictions of breakthrough curves are developed from surface complexation modeling parameters derived from batch sorption data. The influence of goethite specific reactivity on  $\text{Fe}^{\text{II}}$  sorption under batch *vs.* advective-dispersive flow and the mobility of  $\text{Fe}^{\text{II}}$  in the column system are discussed.

## **2. Materials and methods**

### **2.1. Chemicals**

Ferrous chloride tetrahydrate ( $\text{FeCl}_2 \cdot 4\text{H}_2\text{O}$ ) and sodium phosphate ( $\text{Na}_3\text{PO}_4 \cdot 12\text{H}_2\text{O}$ ) were purchased from Sigma Aldrich. Fontainebleau sand (Prolabo) was used.

### **2.2. Goethite samples**

This study involves three different types of goethite which were provided by Dr. F. Gaboriaud (LCPME). These goethites are referred as G1, G2 and G3. These goethites were synthesized and characterized in the context of previous studies by our research group (Gaboriaud and Ehrhardt, 2003; Pr  lot et al., 2003). Briefly, Transmission Electron Microscopy (TEM) and Atomic Force Microscopy (AFM) images showed typical acicular shapes for all goethites samples. The AFM images demonstrated that (101) and/or (001) faces are always dominant on crystallized goethites. The crystal faces (101) and the (001) were identified on the single crystals of G2 and G3, while the main crystallographic faces of G1 particles were found as (001), (101) and (121) or (021) (Gaboriaud and Ehrhardt, 2003; Pr  lot et al., 2003). Their main characteristics including the estimated maximum density of singly coordinated sites per surface unit, and PZC values are summarized in Table 1. The BET surface areas were re-determined in this work and was found almost similar to that determined in previous works ((Gaboriaud and Ehrhardt, 2003; Pr  lot et al., 2003) and Table 1).

Goethite coated sand (GCS) was prepared by using the method reported elsewhere (Scheidegger et al., 1993). Fontainebleau sand (France), with a grain size range of 100-150  $\mu\text{m}$  was used. The mineralogy of the sand was characterized by X-ray diffraction and was found to be exclusively quartz. The quartz sand was cleaned with 1 M HCl for 48 h and then rinsed with pure water. The quartz sand was also cleaned with  $\text{H}_2\text{O}_2$  to remove organic matter and then rinsed with pure water (Hanna, 2007a).

Iron oxides coating was obtained by shaking a suspension containing the iron oxide and the silica sand. The purified quartz sand was then added to the goethite suspension containing 10 mM NaCl brought to pH 5 with HCl and the mixture was agitated again for 24 h. All synthetic solids were washed to remove electrolytes and stored in an anaerobic  $\text{N}_2$  chamber at ambient temperature. X-ray diffraction (XRD) and Raman spectroscopy confirmed that the coating procedure did not alter goethite particles.

Each goethite was deposited on the quartz sand surface to reach an equal amount of goethite ( $0.5 \text{ m}^2$  of goethite per gram of sand). BET surface area measurements and the goethite content of each coated sand as determined by acid digestion analysis, confirmed the desired value. Attachment strength of iron oxide to silica sand was evaluated by shaking suspension of coated sand at pH 3 for 24 h. Amounts of iron in supernatants (after removal of coated sand) before and after acid digestion were then measured. This test showed that the iron oxide was

strongly attached to the silica surface and the percentage of detachment was low enough that its effect could be ignored over experimental conditions (Hanna, 2007a; Tanis et al., 2008).

### 2.3. Batch experiments

The determination of  $\text{Fe}^{\text{II}}$  sorption extent is difficult because sorbent solid (ferric oxyhydroxide) may be transformed into other compounds (e.g. magnetite), via  $\text{Fe}^{\text{II}}$ -to- $\text{Fe}^{\text{III}}$  electron transfer processes. Recent studies have shown that possible transformation of goethite upon  $\text{Fe}^{\text{II}}$  action is slow and requires special conditions such as high  $\text{Fe}^{\text{II}}$  dosage and alkaline pH (Usman et al., 2012a; Usman et al., 2012b; Usman et al., 2013). Therefore sorption of  $\text{Fe}^{\text{II}}$  onto goethite can be normally done at a reasonable time interval and at low  $\text{Fe}^{\text{II}}$  concentration, as described by Liu et al. (Liu et al., 2001). Batch sorption experiments were conducted in a 500 mL polyethylene bottles at 20 °C in a glove box, an anoxic chamber ( $\text{N}_2$ :  $\text{H}_2$  = 98:2) and in the absence of light. The goethite reactive phase concentration was fixed at 50  $\text{m}^2/\text{L}$ , equivalent to a solid-to-liquid ratio of 100 g of GCS per L (0.5  $\text{m}^2/\text{g}$  of GCS)). This high solid-to-liquid ratio (100g GCS/L) was chosen in order to be comparable with the column tests.

The pH of the suspension was maintained by titrating with 0.01M HCl or 0.01M NaOH solutions as required. The sorption of  $\text{Fe}^{\text{II}}$  on three goethites was carried out *vs.* time (0-80 min) at  $\text{pH } 6 \pm 0.1$ . Moreover, sorption of  $\text{Fe}^{\text{II}}$  on three goethites was also evaluated *vs.* pH at a fixed  $\text{Fe}^{\text{II}}$  concentration (0.5 mM). An equilibration period of about 60 min was allowed between each increment, after which a 2 mL sample was taken from the suspension. Before analysis, the suspensions were filtered through 0.22  $\mu\text{m}$  polyvinylidene fluoride (PVDF) syringe filters (Millipore) that were shown not to sorb or oxidize ferrous ion. The filtrates were immediately acidified by using 5 M HCl. The residual  $\text{Fe}^{\text{II}}$  concentration was measured by 1-phenanthroline method at 510 nm on a UV-Vis spectrophotometer. To insure if aqueous  $\text{Fe}^{\text{II}}$  was sorbed and not oxidized by trace amounts of oxygen or other chemical phenomena, mass balance on solid- and aqueous-phase  $\text{Fe}^{\text{II}}$  was conducted for each reactor. Blank tests conducted with uncoated sand showed that the sand did not sorb  $\text{Fe}^{\text{II}}$  under our experimental conditions. The initial concentration of  $\text{Fe}^{\text{II}}$  was determined in parallel reactors without solid. To determine if interparticle diffusion is occurring for sorption of  $\text{Fe}^{\text{II}}$  on goethites, ultrasonic mixing was used in order to disperse loosely formed aggregates in the solution. The sorption rate constants obtained with ultrasonication and magnetic stirring were, then, compared.

Additional batch experiments were conducted in glove box to test the impact of surface-sorbed phosphate on the sorption and uptake of  $\text{Fe}^{\text{II}}$  by goethite surface. Phosphate was chosen as model compound because it is representative of naturally occurring inorganic ligands and it forms strong inner sphere complexes with the iron oxide surface. Phosphate was pre-sorbed to the goethite, and  $\text{Fe}^{\text{II}}$  (0.1 mM) was added subsequently to the goethite/phosphate suspension containing 10  $\text{m}^2/\text{L}$  of goethite and 0.1 mM of phosphate. These conditions were chosen to avoid precipitation of vivianite and achieve the theoretical maximum for surface adsorption of  $\sim 2.5 \mu\text{mol}/\text{m}^2$  (Torrent et al., 1990; Strauss et al., 2005).

## 2.4. Sorption breakthrough column experiments

Column studies were conducted in duplicate to evaluate the sorption behavior under flow-through conditions. GCS was dry packed into glass chromatographic columns (20 cm long, 1.6 cm internal diameter; XK 16, GE Healthcare). The porous bed had a length of 6 cm and a dry mass of about 20 g (equivalent to 10  $\text{m}^2$  of goethite). After packing to a uniform bulk density ( $1.65 \pm 0.01 \text{ g}/\text{cm}^3$ ), the column was wetted upward with a background electrolyte solution ( $\text{NaCl}$ ,  $10^{-2} \text{ mol}/\text{L}$ ) at a constant flow rate. Once the column was water saturated, a non-reactive tracer experiment was performed in order to identify the flow characteristics through the column. The column was fed upwards at the same constant flow rate with the tracer solution composed of potassium bromide at  $10^{-2} \text{ mol}/\text{L}$  in a pulse mode: injection of 1 mL of tracer solution followed by background solution. Bromide concentrations were measured by ion chromatography.

Aqueous transport can be characterized from the analysis of tracer experiments. The pulse injection of bromide induces a bell shaped elution curve characterized by a slight asymmetrical shape with little tailing (data not shown). Solutes were transported through water-driven convection and dispersion, thereby ensuring contact with all particles contacted by interstitial waters. The data analysis was carried out with the method of moments and the advective–dispersive model. The classical convection dispersion equation (CDE) generally describes accurately the 1D transport of a non-reactive solute under steady-state water flow in a saturated column:

$$\frac{\partial C}{\partial t} = D \frac{\partial^2 C}{\partial x^2} - v \frac{\partial C}{\partial x} \quad (1)$$



where  $c$  denotes the water solute concentration ( $M/L^3$ ),  $t$  is time (T),  $x$  the spatial coordinate (L),  $D$  the dispersion coefficient ( $L^2/T$ ),  $v$  the flow velocity (L/T),  $\theta$  the porosity ( $L^3/L^3$ ), and  $q$  the darcian velocity (L/T). The concentration of non-reactive solute in the outflow was analyzed using CDE developed on MATHCAD software to obtain the values of the hydrodynamic parameters  $\theta$  and  $D$ . The fit of bromide elution curve provided estimations of  $\theta$  and  $D$  that characterize of flow homogeneity (Sardin et al., 1991). Modeling with the MIM code (mobile immobile water) that considers a mobile zone where flow is allowed, an immobile zone with no flow, and exchange of solute between the two zones by diffusion, did not improve the fit. Also, the estimate for immobile water was negligibly low. These results thus indicate that the classical advection-dispersion model (ADE) (Eq. 1) is sufficient to describe solute transport in the GCS-packed column.

The dispersivity  $\alpha$  (L) was calculated neglecting molecular diffusion, according to:

$$\alpha = \frac{D}{v} \quad (2)$$

The Darcy velocity ( $q$ ), porosity  $\theta$ ,  $v$  (pore water velocity),  $D$  (dispersion coefficient) are reported in Table 2. The dispersivity  $\alpha$  was around 105  $\mu m$ , close to the grain size particle (100-150  $\mu m$ ). The Péclet number ( $Pe = vL/D$ ) in the column was higher than 500, indicating the predominance of an advective regime in all columns (Table 2).

Column experiments were performed to predict the impact of goethite type on the mobility of  $Fe^{II}$  in GCS column. The column was injected with  $Fe^{II}$  solution (0.5 mM, dissolved form) at pH 6 in a continuous mode at the same constant flow rate, in a glove box. For this purpose, the column was carefully evacuated and flushed with  $N_2$  to remove as much oxygen as possible. The column was then slowly saturated by upward flow of the degassed background solution. The porosity and pore volume was determined gravimetrically, and the injected solution was flushed continuously with a  $N_2$  gas. During water saturation and tracer experiments, total Fe in outflow was almost negligible, and therefore possibility of dissolution and dispersion of goethite particles is excluded from the column throughout the course of the experiment.

The flow-through experiments were duplicated for each goethite column. In order to study the impact of non-equilibrium sorption in the G1-containing column, two lower flow rates (0.1 and 0.5 mL/min) were used to ensure greater column residence times. Dissolved  $Fe^{II}$  and total Fe concentrations in the collected fractions were measured by 1-phenanthroline method (UV – visible spectrophotometry).

## 2.5. Surface complexation modeling

The double layer model (DLM) (Dzombak and Morel, 1990) investigated by Dixit and Hering (2006) was used here to describe the  $\text{Fe}^{\text{II}}$  sorption vs. pH. This DLM is implemented in PHREEQC2 code (Parkhurst and Appelo, 1999; Hanna, 2007b). The protonation constants of the surface hydroxyl groups and surface parameters previously determined in (Gaboriaud and Ehrhardt, 2003; Pr  lot et al., 2003) were used to predict  $\text{Fe}^{\text{II}}$  sorption onto goethite. All calculations were carried out using the constants listed in Table 1.

PHREEQC-2 was also used to calculate species transport in the GCS-packed column (Rusch et al., 2010). This program enables calculation of chemical equilibria, including different types of interaction of dissolved species with solid phases, in combination with one dimensional conservative advective dispersive mass transport. The specific transport procedure and solute concentration calculations in PHREEQC2 are explained elsewhere (Parkhurst and Appelo, 1999; Hanna et al., 2010; Rusch et al., 2010).

## 3. Results and discussion

### 3.1. Sorption of $\text{Fe}^{\text{II}}$ in batch experiments

#### 3.1.1. Kinetic results

The kinetics data obtained under batch conditions revealed that  $\text{Fe}^{\text{II}}$  uptake reached a steady state at 30 min for G2 and G3, and at around 60 min for G1 (Fig.1a). Different kinetic models, namely a pseudo-first-order, a pseudo-second-order and an intraparticle diffusion model were applied to the data. One way to assess the goodness of fit of experimental kinetic data to these equations is to check the regression coefficients obtained during the regression analysis. The pseudo first-order expression provided the best fit, whereas the pseudo-second-order and the intraparticle diffusion models did not fit well the data. Sorption data were, therefore, treated according to the first-order kinetics by plotting  $\ln(Q_e/Q_e - Q_t)$  as a function of time,  $t$ , and applying linear regression analysis to obtain the rate constant according to the following equation:

$$\ln \frac{Q_e}{Q_e - Q_t} = kt \quad (3)$$

where  $Q_e$  and  $Q_t$  ( $\mu\text{mol}/\text{m}^2$ ) are the amount of sorption at equilibrium and at time  $t$  (min), respectively and  $k$  is the rate constant of the first order sorption process. The order of the

kinetic rate constants ( $\text{min}^{-1}$ ) can be classified as  $G2 (0.094) > G3 (0.070) > G1 (0.052)$ . G1 exhibited the slowest sorption reaction rate, which could be due to the heterogeneity of the surface site bonding energy or because of other chemical reactions occurring on the surface (Liger et al., 1999; Dixit and Hering, 2006; Hiemstra and van Riemsdijk, 2007). As largely stated in literature, the interactions of aqueous  $\text{Fe}^{\text{II}}$  with iron oxides can produce a variety of reactions including sorption, electron transfer, dissolution and atom exchange, and so it is difficult to argue that all these processes might be described by a first-order equation (Williams and Scherer, 2004; Pedersen et al., 2005; Larese-Casanova and Scherer, 2007; Handler et al., 2009).

The sorption results with both ultrasonication and magnetic stirring are almost the same, suggesting that interparticle diffusion is not the rate-limiting step. In all cases, mass balance on solid- and aqueous-phase  $\text{Fe}^{\text{II}}$  was determined, and showed that  $\text{Fe}^{\text{II}}$  was removed only by sorption while no oxidation by trace amounts of oxygen or other phenomena occur.

### 3.1.2. Sorption vs. pH

The effect of varying solution pH on the sorption of  $\text{Fe}^{\text{II}}$  is illustrated in Figure 1b. The shape of the sorption envelopes is consistent with cationic species interacting with the oxide surfaces (Liger et al., 1999; Dixit and Hering, 2006; Hiemstra and van Riemsdijk, 2007, and references cited within). The observed sorption behavior can be attributed to a combination of pH-dependent speciation of ferrous ion and surface charge characteristics of the mineral oxide. Based upon surface charge, sorption is negligible at low pH values and then increases with an increase in pH. The effect of varying pH on  $\text{Fe}^{\text{II}}$  sorption is similar for all goethites, although G1 exhibits a higher sorption extent than G2 or G3. These observations are consistent with literature (Liger et al., 1999; Hiemstra and van Riemsdijk, 2007) which reported that the sorption of  $\text{Fe}^{\text{II}}$  onto iron oxyhydroxide phases increases strongly at a pH higher than 7 regardless of the tested iron oxide.

In order to describe the sorption data vs. pH, surface complexation modeling (SCM) incorporated in PHREEQC2 was used. According to previous works (Dixit and Hering, 2006; Hiemstra and van Riemsdijk, 2007),  $\text{Fe}^{\text{II}}$  sorption in the goethite/water interface can be best described by assuming two surface complexes with and without electron transfer. The equations predicting  $\text{Fe}^{\text{II}}$  sorption at low  $\text{Fe}^{\text{II}}$  concentration on goethite are shown in Table 3. These equations are based on the work of Dixit and Hering (2006) who proposed two monodenate mononuclear reactions implying one type of site with a positively charged

surface species and an uncharged surface species. The relative contribution of each equation varies as a function of pH where the sorption of  $\text{Fe}(\text{OH})^+$  is more pH dependent than that of  $\text{Fe}^{2+}$  (Dixit and Hering, 2006).

Surface complexation constants of the equations 1 and 2 were obtained by fitting the experimental data vs. pH (Table 3, Fig.1b). The experimental data for all three goethites were successfully described by using the same surface complexation constant values, only the site density value was changed (Table 2). These values of site density are, however, different from those previously determined by considering maximum site density per crystal face present in each goethite (Table 1 and references (Gaboriaud and Ehrhardt, 2003; Pr  lot et al., 2003)).

### *3.1.3. Effect of phosphate adsorption*

The impact of sorbed phosphate on the sorption and uptake of  $\text{Fe}^{\text{II}}$  by goethite surface was tested by presorbing phosphate to the goethite and then adding aqueous  $\text{Fe}^{\text{II}}$  to the suspension. The three goethites were used at the same exposed surface area per volume unit (i.e.  $10 \text{ m}^2/\text{L}$ ) and the total phosphate loading was  $10 \text{ }\mu\text{mol}/\text{m}^2$ . In these conditions, no significant  $\text{Fe}^{\text{II}}$  sorption was observed for all goethites, suggesting that phosphate strongly affects the  $\text{Fe}^{\text{II}}$  sorption on the goethite surface.

Phosphate binds strongly to  $\text{Fe}^{\text{III}}$ -oxides through monodentate and/or multidentate-mononuclear surface complexes (Torrent et al., 1990; Luengo et al., 2006), decreasing significantly the availability of surface sites. These results are consistent with the findings of previous works where phosphate was found to interfere with the  $\text{Fe}^{\text{II}}$  induced recrystallisation of ferric oxyhydroxides (Benali et al., 2001; Borch et al., 2006; Usman et al., 2013). However, recent study (Latta et al., 2012) showed that both  $\text{Fe}^{\text{II}}$ -  $\text{Fe}^{\text{III}}$  electron transfer and Fe atom exchange are unaffected by phosphate sorption on goethite by investigating  $^{57}\text{Fe}$  M  ssbauer spectroscopy and isotope tracer method. These contradictory results may result from the difference in the experimental conditions used (e.g. exposed surface area per volume unit, ratio P/Fe, etc.) and also in the nature of the underlying goethite. Indeed, phosphate sorption has been tested on eight samples of goethite ranging in surface area from 18 to  $132 \text{ m}^2/\text{g}$  and concluded that the duration and extent of the sorption reaction depended on the crystallinity of the goethite (Strauss et al., 2005). Torrent et al. (1990) have observed that the amount of phosphate adsorbed per unit surface area at pH of 6 was similar for all tested goethites ( $2.51 \text{ }\mu\text{mol}/\text{m}^2$ ), because of the existence of only (110) faces in their goethite samples. They, however stated that the crystal morphology affected desorption extents, since samples

consisting of multidomainic laths retain more phosphate than those having monodomainic crystals (Torrent et al., 1990). Therefore, the impact of strongly bonded ligand on the  $\text{Fe}^{\text{II}}$  sorption also points out the importance of morphology, crystal structure and particle size of the underlying goethite surface.

### 3.2. Sorption and transport of $\text{Fe}^{\text{II}}$ in column

#### 3.2.1. Sorption of $\text{Fe}^{\text{II}}$ in columns

Column experiments were performed under conditions to predict the impact of goethite type on the mobility of  $\text{Fe}^{\text{II}}$  in GCS column. The breakthrough curves (BTC) of both pH and aqueous  $\text{Fe}^{\text{II}}$  are shown for each goethite in Figure 2, while those of aqueous  $\text{Fe}^{\text{II}}$  only are regrouped for the three goethites in Figure 3a. The breakthrough point of Fe from G3 and G2 lies respectively at about 4 and 5  $\text{V}/\text{V}_\text{p}$ , while complete breakthrough occurs at  $\sim 7$  injected pore volumes (PV). The total sorbed amount of  $\text{Fe}^{\text{II}}$  at complete breakthrough is  $\sim 1.1$  and  $1.3 \mu\text{mol}/\text{m}^2$  for G3 and G2 respectively, which is in agreement with that expected from the batch experiments.

The breakthrough point for G1 column starts at  $\sim 6$  PV and is completed at  $\sim 10$  PV.  $\text{Fe}^{\text{II}}$  surface loading ( $\sim 1.6 \mu\text{mol}/\text{m}^2$ ) is, however, less than derived from batch sorption experiments (Fig.1). The pH coincides with the  $\text{Fe}^{\text{II}}$  breakthrough slope and reaches a constant value when solute sorption achieves steady state and breakthrough completion (Fig.2).

Additional breakthrough experiments were conducted by injecting aqueous  $\text{Fe}^{\text{II}}$  solution in columns containing dried GCS-sorbed phosphate. Prior to column experiments, preliminary batch tests were conducted to prepare the GCS by mixing 20 g of GCS (equivalent to  $10 \text{ m}^2$  of goethite) with 0.1 mM of phosphate solution (total ligand loading  $10 \mu\text{mol}/\text{m}^2$ ). The breakthrough curves of  $\text{Fe}^{\text{II}}$  superposed with that of bromide tracer (Fig. 3a), and thus no  $\text{Fe}^{\text{II}}$  sorption occurred in the column whatever the goethite used. These results confirm those observed in batch, *i.e.* phosphate hinders the adsorption sites and therefore inhibits the  $\text{Fe}(\text{II})$  sorption.

Transport modeling was carried out with PHREEQC2, using hydrodynamic parameters defined by a  $\text{Br}^-$  tracer breakthrough experiment and the surface complexation parameters of this study (Table 2).  $\text{Fe}^{\text{II}}$  sorption in dynamic conditions (columns) can be satisfactorily predicted by coupling aqueous transport (convection and dispersion) and the surface complexation model (batch experiments) for the G2 and G3 columns (solid lines in Fig.3a). The predicted breakthrough, however, overestimated Fe sorption in the G1 column system

and showed a larger retardation (Fig.3a). Indeed, experimental breakthrough was at about 6 PV, while calculations predicted around 8 PV.

The inability of the model simulation of a laboratory column experiment to describe outflow concentrations could possibly be related to the lack of local geochemical equilibrium in the column (Altfelder et al., 2001; Hanna and Boily, 2010). The comparison of sorption kinetic rate and the residence time in the column at 1 ml/min (about 5 min) as well as the short tail observed in the BTC suggests that kinetic limitations of sorption might take place in the column. While BTC of G1 exhibits less dispersion on the initial limb, the tailing observed on desorption limb may be an indication of a kinetics effect and/or dispersion effect.

Firstly, when solute BTCs normalized by its retardation factor was compared to that of the Br<sup>-</sup> tracer, BTC was more tilted than that of the tracer (not shown). This observation is in favor of nonequilibrium sorption in the column. In contrast, if there is no influence of sorption kinetics, the steepness of the solute BTC is determined only by dispersion and must coincide with the tracer BTC. Another way to test the lack of local equilibrium is by estimating the Damkohler numbers (Da), representing the ratio of hydrodynamic residence time to characteristic time for sorption of a compound, as described elsewhere (Bi et al., 2009; Hanna and Boily, 2010; Hanna et al., 2010; Clervil et al., 2013).  $Da = \tau(R-1)L/v$ , where  $\tau$  is the mass transfer coefficient estimated from batch kinetic experiment ( $0.052 - 0.094 \text{ min}^{-1}$ ), R is retardation factor estimated from moment analysis of the breakthrough curves, L is the column length (cm) and  $v$  is the average pore water velocity ( $\text{cm min}^{-1}$ ). Da values varied between 1.5 (G1), 2 (G2) and 1.6 (G3) inferior to 20. Consequently, lower values of Da are not in favor of local equilibrium in a 1-D column (Maraqa et al., 1998; Bi et al., 2009).

### 3.2.2. Sorption of $\text{Fe}^{\text{II}}$ in the G1 column at different pore water velocities

The best experimental method for testing the impact of kinetics in a packed column is to conduct the breakthrough experiment at different flow rates or residence times. For this aim, flow-through experiments were conducted at three different flow rates ( $0.1, 0.5$  and  $1 \text{ ml min}^{-1}$ ) at pH 6 for the G1 packed column (Fig. 3b). Interestingly, breakthrough curves were found to be dependent on flow rates, indicating that the sorption kinetics impact  $\text{Fe}^{\text{II}}$  transport over the time scale of column experiment. The three sets of flow-through experiments gave rise to different retardation factors at complete breakthrough. The breakthrough curves at 1 and  $0.5 \text{ ml/min}$  were sigmoidal in shape and showed no extended tailing; however the BTC at the lowest flow rate ( $0.1 \text{ ml/min}$ ) exhibits an irregular shape (Fig. 3b). This behavior observed at

a high residence time (about 50 min) might come from Fe dissolution/re-precipitation or  $\text{Fe}^{\text{II}}$ -induced transformation of goethite. Note that the dissolved ferrous ion can be flushed out under flow-through conditions, which could modify the extent of reaction in the column and explain the irregular shape of the BTC (Fig. 3b). However, XRD or Raman spectroscopy conducted on the goethite coated sand before and after column test did not show any significant difference (data not shown). As the  $\text{Fe}^{\text{III}}$  loading in GCS (less than 1 wt%) is very low as well as the  $\text{Fe}^{\text{II}}$  binding amount, a detection of mineralogical transformation of goethite or an identification of secondary minerals is quite difficult. Note that this degree of coating was chosen to correspond to the Fe oxide coatings range (0.074 to 44.2 mg Fe by gram of sand) found in natural settings (Wang et al., 1993), and also help to do column experiments in a reasonable period of time.

Based upon these results, transport of  $\text{Fe}^{\text{II}}$  in goethite packed column was found dependent on time scale especially in the G1 system. Despite the agreement observed between batch and column data in term of sorbed amount (at low flow rate), we cannot suppose that the equilibrium is established in the column.

In our previous reports on the transport of organic ligands in GCS columns, compatibility of batch and column methods was found strongly dependent on ligand structure, sorbent nature and sorption mechanism (Hanna and Boily, 2010; Hanna et al., 2010; Rusch et al., 2010). In present work, we can imagine that the disparity between batch and column data may also result from the modification of sorption process and/or surface properties under flow through conditions. However, it is difficult to test these hypotheses here due to the complexity of interactions between  $\text{Fe}^{\text{II}}$  and iron oxide (sorption with or without electron transfer, possible transformation to secondary minerals, etc.). Moreover, the goethite content in columns is too low to allow a relevant characterization and monitoring of iron reactive phases.

In order to test if the observed disparity resulted from the specific interactions of  $\text{Fe}^{\text{II}}$  with  $\text{Fe}^{\text{III}}$  oxide, BTCs were determined as for previous experiments but by using fluoride as a reactive tracer. Fluoride was used as a model compound because the interactions of fluoride with iron oxides have been largely described in literature (Sigg and Stumm, 1981). The breakthrough results showed that, like the  $\text{Fe}^{\text{II}}$ , the disparity between batch and column data was only observed for G1. This observation indicates that this behavior is directly related to the specific phase reactivity of the used goethite (*i.e.* G1). In our batch experiments, G1 has the highest sorption extent and lowest sorption rate constant.

Under batch conditions, kinetic data of  $\text{Fe}^{\text{II}}$  sorption suggested some heterogeneity of chemical reactions occurring on the G1 surface. The high sorption capability of G1 might have resulted from the surface roughness and edge surface faces enhancing surface site densities. Manceau et al. (2000) suggested that the sorption of divalent cations may probably be dominated by the crystal faces that terminate the chains (021/001 like faces) and the presence of the face 021 or 121 favored the formation of bidentate or tridentate complex. Therefore, the presence of the edges faces, as in the case of G1 (Gaboriaud and Ehrhardt, 2003; Pr  lot et al., 2003), might favor the formation of inner-sphere complex, making the  $\text{Fe}^{\text{II}}$  sorption stronger.

In addition, longer residence time in the breakthrough experiments allowed for greater sorption and dispersion with an unusual breakthrough shape. Appelo and Postma (1999) suggested that chemical reactions inside column can induce changes in the pore structure and then influence the flow properties of media, since they observed 10-fold increase in dispersion due to the reduction of the sorbent solid by  $\text{Fe}^{\text{II}}$  in the column system.

All these observations suggest that the strong  $\text{Fe}^{\text{II}}$  sorption on G1 makes it kinetically limited under flow through conditions. Therefore, the crystal structure and surface site density of goethite are needed to describe and predict the transport of  $\text{Fe}^{\text{II}}$  in column.

#### **4. Implications for contaminant attenuation and transport**

Sorption of  $\text{Fe}^{\text{II}}$  onto iron oxide minerals plays an important role both in natural and engineered systems. Sorption of  $\text{Fe}^{\text{II}}$  to the iron oxides has possible consequences on the fate of contaminants in the environment. On the one hand, presence of  $\text{Fe}^{\text{II}}$  in a goethite suspension can induce increases in sorption of metal cations (Coughlin and Stone, 1995). On the other hand,  $\text{Fe}^{\text{II}}$  associated with goethite or other  $\text{Fe}^{\text{III}}$ -hydroxide surfaces was shown to be a very powerful reductant of several environmental contaminants (Elsner et al., 2004). The rate and extent of contaminant reduction depends on the composition of the mineral, amount of  $\text{Fe}^{\text{II}}$  sorbed, and possibly the speciation of sorbed  $\text{Fe}^{\text{II}}$  (Hofstetter et al., 1999; Elsner et al., 2004; Tobler et al., 2007; Usman et al., 2012a). We notably demonstrated that the sorption of  $\text{Fe}^{\text{II}}$  on goethite is strongly affected by the specific surface properties of the underlying phase.

In addition, the mobility of  $\text{Fe}^{\text{II}}$  under anoxic flow conditions was dependent on the goethite phase. For two goethites G2 and G3, sorption breakthrough predictions using sorption



parameters derived from batch experiments accurately predicted mobility of  $\text{Fe}^{\text{II}}$ . Those for G1, however, predicted less sorption reactions than in the batch sorption experiments. Additional breakthrough experiments and test calculations showed that these differences were related to kinetics behavior. Therefore, the effect of sorption kinetics was especially observed in the G1 column. The specific properties of G1 (i.e. surface roughness, edge surface faces, high site density) leading to a high sorption extent and a low sorption rate, may affect the transport and mobility of aqueous  $\text{Fe}^{\text{II}}$  in the column system.

The dependence of transport of  $\text{Fe}^{\text{II}}$  on the type of goethite phase under advective-flow conditions raise important consequences in prediction mobility models. This aspect should be taken into account in transport and attenuation studies of environmental contaminants.

**Acknowledgment.** We gratefully acknowledge Dr. F. Gaboriaud for providing the three goethites samples and G. Ollivier for XRD analyses.

## References

- Altfelder, S., Streck, T., Maraqa, M.A., Voice, T.C., 2001. Nonequilibrium sorption of dimethylphthalate - Compatibility of batch and column techniques. *Soil Sci. Soc. Am. J.* 65, 102-111.
- Amstaetter, K., Borch, T., Larese-Casanova, P., Kappler, A., 2009. Redox transformation of arsenic by Fe (II)-activated goethite ( $\alpha$ -FeOOH). *Environ. Sci. Technol.* 44, 102-108.
- Appelo, C.A.J., Postma, D., 1999. Variable dispersivity in a column experiment containing MnO<sub>2</sub> and FeOOH-coated sand. *J. Contam. Hydrol.* 40, 95-106.
- Benali, O., Abdelmoula, M., Refait, P., Génin, J.-M.R., 2001. Effect of orthophosphate on the oxidation products of Fe(II)-Fe(III) hydroxycarbonate: the transformation of green rust to ferrihydrite. *Geochim. Cosmochim. Acta* 65, 1715-1726.
- Bi, E., Zhang, L., Schmidt, T.C., Haderlein, S.B., 2009. Simulation of nonlinear sorption of N-heterocyclic organic contaminants in soil columns. *J. Contam. Hydrol.* 107, 58-65.
- Borch, T., Masue, Y., Kukkadapu, R.K., Fendorf, S., 2006. Phosphate Imposed Limitations on Biological Reduction and Alteration of Ferrihydrite. *Environ. Sci. Technol.* 41, 166-172.
- Clervil, E., Usman, M., Emmanuel, E., Chatain, V., Hanna, K., 2013. Sorption of nalidixic acid onto sediments under batch and dynamic flow conditions. *Chem. Geol.* 335, 63-74.
- Cornell, R.M., Schwertmann, U., 1996. *The Iron Oxides: Structure, Properties, Reactions, Occurrence and Uses*, Second ed. Wiley-VCH.
- Coughlin, B.R., Stone, A.T., 1995. Nonreversible adsorption of divalent metal ions (MnII, CoII, NiII, CuII, and PbII) onto goethite: effects of acidification, FeII addition, and picolinic acid addition. *Environ. Sci. Technol.* 29, 2445-2455.
- Dixit, S., Hering, J.G., 2006. Sorption of Fe(II) and As(III) on goethite in single- and dual-sorbate systems. *Chem. Geol.* 228, 6-15.
- Dzombak, D.A., Morel, F.M., 1990. *Surface Complexation Modeling: Hydrous Ferric Oxide*. John Wiley & Sons, New York.
- Elsner, M., Schwarzenbach, R.P., Haderlein, S.B., 2004. Reactivity of Fe(II)-Bearing Minerals toward Reductive Transformation of Organic Contaminants. *Environ. Sci. Technol.* 38, 799-807.
- Gaboriaud, F., Ehrhardt, J.-J., 2003. Effects of different crystal faces on the surface charge of colloidal goethite ( $\alpha$ -FeOOH) particles: an experimental and modeling study. *Geochim. Cosmochim. Acta* 67, 967-983.
- Handler, R.M., Beard, B.L., Johnson, C.M., Scherer, M.M., 2009. Atom exchange between aqueous Fe (II) and goethite: An Fe isotope tracer study. *Environ. Sci. Technol.* 43, 1102-1107.
- Hanna, K., 2007a. Adsorption of aromatic carboxylate compounds on the surface of synthesized iron oxide-coated sands. *Appl. Geochem.* 22, 2045-2053.
- Hanna, K., 2007b. Sorption of two aromatic acids onto iron oxides: Experimental study and modeling. *J. Colloid Interf. Sci.* 309, 419-428.
- Hanna, K., Boily, J.F., 2010. Sorption of two naphthoic acids to goethite surface under flow through conditions. *Environ. Sci. Technol.* 44, 8863-8869.
- Hanna, K., Rusch, B., Lassabatere, L., Hofmann, A., Humbert, B., 2010. Reactive transport of gentisic acid in a hematite-coated sand column: Experimental study and modeling. *Geochim. Cosmochim. Acta* 74, 3351-3366.
- Hiemstra, T., van Riemsdijk, W.H., 2007. Adsorption and surface oxidation of Fe(II) on metal (hydr)oxides. *Geochim. Cosmochim. Acta* 71, 5913-5933.

Hofstetter, T.B., Heijman, C.G., Haderlein, S.B., Holliger, C., Schwarzenbach, R.P., 1999. Complete reduction of TNT and other (poly) nitroaromatic compounds under iron-reducing subsurface conditions. *Environ. Sci. Technol.* 33, 1479-1487.

Larese-Casanova, P., Scherer, M.M., 2007. Fe (II) sorption on hematite: New insights based on spectroscopic measurements. *Environ. Sci. Technol.* 41, 471-477.

Latta, D.E., Bachman, J.E., Scherer, M.M., 2012. Fe Electron Transfer and Atom Exchange in Goethite: Influence of Al-Substitution and Anion Sorption. *Environ. Sci. Technol.* 46, 10614-10623.

Liger, E., Charlet, L., Van Cappellen, P., 1999. Surface catalysis of uranium(VI) reduction by iron(II). *Geochim. Cosmochim. Acta* 63, 2939-2955.

Liu, C., Kota, S., Zachara, J.M., Fredrickson, J.K., Brinkman, C.K., 2001. Kinetic Analysis of the Bacterial Reduction of Goethite. *Environ. Sci. Technol.* 35, 2482-2490.

Luengo, C., Brigante, M., Antelo, J., Avena, M., 2006. Kinetics of phosphate adsorption on goethite: Comparing batch adsorption and ATR-IR measurements. *J. Colloid Interf. Sci.* 300, 511-518.

Manceau, A., Nagy, K.L., Spadini, L., Ragnarsdottir, K.V., 2000. Influence of Anionic Layer Structure of Fe-Oxyhydroxides on the Structure of Cd Surface Complexes. *J. Colloid Interf. Sci.* 228, 306-316.

Maraqa, M.A., Zhao, X., Wallace, R.B., Voice, T.C., 1998. Retardation coefficients of nonionic organic compounds determined by batch and column techniques. *Soil Sci. Soc. Am. J.* 62, 142-152.

Parkhurst, D.L., Appelo, C.A.J., 1999. User's guide to PHREEQC (Version 2) a computer program for speciation, batch-reaction, one-dimensional transport, and inverse geochemical calculations: U.S. Geological Survey Water-Resources Investigations Report pp. 99-4259.

Pedersen, H.D., Postma, D., Jakobsen, R., Larsen, O., 2005. Fast transformation of iron oxyhydroxides by the catalytic action of aqueous Fe(II). *Geochim. Cosmochim. Acta* 69, 3967-3977.

Prélot, B., Villiéras, F., Pelletier, M., Gérard, G., Gaboriaud, F., Ehrhardt, J.-J., Perrone, J., Fedoroff, M., Jeanjean, J., Lefèvre, G., Mazerolles, L., Pastol, J.-L., Rouchaud, J.-C., Lindecker, C., 2003. Morphology and surface heterogeneities in synthetic goethites. *J. Colloid Interf. Sci.* 261, 244-254.

Rusch, B., Hanna, K., Humbert, B., 2010. Sorption and Transport of Salicylate in a Porous Heterogeneous Medium of Silica Quartz and Goethite. *Environ. Sci. Technol.* 44, 2447-2453.

Sardin, M., Schweich, D., Leij, F.J., Van Genuchten, M.T., 1991. Modeling the nonequilibrium transport of linearly interacting solutes in porous media: A review. *Water Resour. Res.* 27, 2287-2307.

Scheidegger, A., Borkovec, M., Sticher, H., 1993. Coating of silica sand with goethite: preparation and analytical identification. *Geoderma* 58, 43-65.

Schwertmann, U., Cornell, R.M., 2000. *Iron Oxides in the Laboratory: Preparation and Characterization*. Wiley-VCH, New York.

Sigg, L., Stumm, W., 1981. The interaction of anions and weak acids with the hydrous goethite ( $\text{FeOOH}$ ) surface. *Colloid. Surface.* 2, 101-117.

Strauss, R., Brümmer, G.W., Barrow, N.J., 2005. Effects of crystallinity of goethite: II. Rates of sorption and desorption of phosphate. *Eur. J. Soil Sci.* 48, 101-114.

Stumm, W., Sulzberger, B., 1992. The cycling of iron in natural environments: Considerations based on laboratory studies of heterogeneous redox processes. *Geochim. Cosmochim. Acta* 56, 3233-3257.

Tanis, E., Hanna, K., Emmanuel, E., 2008. Experimental and modeling studies of sorption of tetracycline onto iron oxides-coated quartz. *Colloid. Surface. A* 327, 57-63.

Tobler, N.B., Hofstetter, T.B., Schwarzenbach, R.P., 2007. Assessing Iron-Mediated Oxidation of Toluene and Reduction of Nitroaromatic Contaminants in Anoxic Environments Using Compound-Specific Isotope Analysis. *Environ. Sci. Technol.* 41, 7773-7780.

Torrent, J., Barron, V., Schwertmann, U., 1990. Phosphate adsorption and desorption by goethites differing in crystal morphology. *Soil Sci. Soc. Am. J.* 54, 1007-1012.

Usman, M., Abdelmoula, M., Faure, P., Ruby, C., Hanna, K., 2013. Transformation of various kinds of goethite into magnetite: Effect of chemical and surface properties. *Geoderma* 197-198, 9-16.

Usman, M., Abdelmoula, M., Hanna, K., Grégoire, B., Faure, P., Ruby, C., 2012a. FeII induced mineralogical transformations of ferric oxyhydroxides into magnetite of variable stoichiometry and morphology. *J. Solid State Chem.* 194, 328-335.

Usman, M., Hanna, K., Abdelmoula, M., Zegeye, A., Faure, P., Ruby, C., 2012b. Formation of green rust via mineralogical transformation of ferric oxides (ferrihydrite, goethite and hematite). *Appl. Clay Sci.* 64, 38-43.

Wang, H.D., White, G.N., Dixon, J.B., Turner, F.T., 1993. Ferrihydrite, lepidocrocite, and goethite in coatings from east Texas vertic soils. *Soil Sci. Soc. Am. J.* 57, 1381-1386.

Williams, A.G.B., Scherer, M.M., 2004. Spectroscopic Evidence for Fe(II)-Fe(III) Electron Transfer at the Iron Oxide-Water Interface. *Environ. Sci. Technol.* 38, 4782-4790.

## Tables

**Table 1. Main characteristics of tested goethites (G1, G2 and G3) (Gaboriaud and Ehrhardt, 2003; Prélôt et al., 2003).**

	G1	G2	G3
BET surface area (m <sup>2</sup> /g)	40	51	93
Particle size (nm)	300-400	200-300	100-200
Point of zero charge (PZC)	9.0	9.0	9.1
Estimated singly coordinated site density (sites/nm <sup>2</sup> )	3.59	3.07	3.03

**Table 2. Characteristics of column experiments with three goethites (G1, G2 and G3)**

	G1	G2	G3
Porous bed length (cm)	6 ± 0.2	6 ± 0.2	6 ± 0.2
Section (cm <sup>2</sup> )	2.01	2.01	2.01
Column volume (cm <sup>3</sup> )	12.06	12.06	12.06
GCS amount (g)	20 ± 1	20 ± 1	20 ± 1
Bulk density (g.cm <sup>-3</sup> )	1.65 ± 0.1	1.65 ± 0.1	1.65 ± 0.1
Experimental V <sub>p</sub> (ml)	4.5±0.2	4.5±0.2	4.5±0.2
Porosity (%)	0.37	0.37	0.37
Flow rate (mL/min)	1.00	1.00	1.00
Darcy velocity (cm/min)	0.50	0.50	0.50
Pore-water velocity (cm/min)	1.35	1.35	1.35
D cm <sup>2</sup> /min	0.015	0.014	0.014
α μm	111	104	104
Pe	540	580	580

**Table 3.** Equilibrium constants and intrinsic surface complexation constants used in the sorption modeling.

Reaction	G1	G2	G3
Surface acid-base reactions			
$\equiv\text{FeOH} \rightleftharpoons \equiv\text{FeO}^- + \text{H}^+$	-10.3	-10.3	-10.4
$\equiv\text{FeOH} + \text{H}^+ \rightleftharpoons \equiv\text{FeOH}^{2+}$	7.6	7.6	7.8
Fe <sup>II</sup> sorption reactions			
$\equiv\text{Fe}^{\text{III}}\text{OH} + \text{Fe}^{2+} \rightleftharpoons (\equiv\text{Fe}^{\text{III}}\text{OFe}^{\text{II}})^+ + \text{H}^+$	-0.1	-0.1	-0.1
$\equiv\text{Fe}^{\text{III}}\text{OH} + \text{Fe}^{2+} + \text{H}_2\text{O} \rightleftharpoons (\equiv\text{Fe}^{\text{II}}\text{OFe}^{\text{III}}\text{OH})^0 + 2\text{H}^+$	-11.3	-11.3	-11.3
Surface site density [ $\equiv\text{FeOH}$ ] <sub>tot</sub> for 50 m <sup>2</sup> /L	0.5 mM 10 μmol/m <sup>2</sup>	0.3 mM 6 μmol/m <sup>2</sup>	0.2 mM 4 μmol/m <sup>2</sup>

## Figures captions

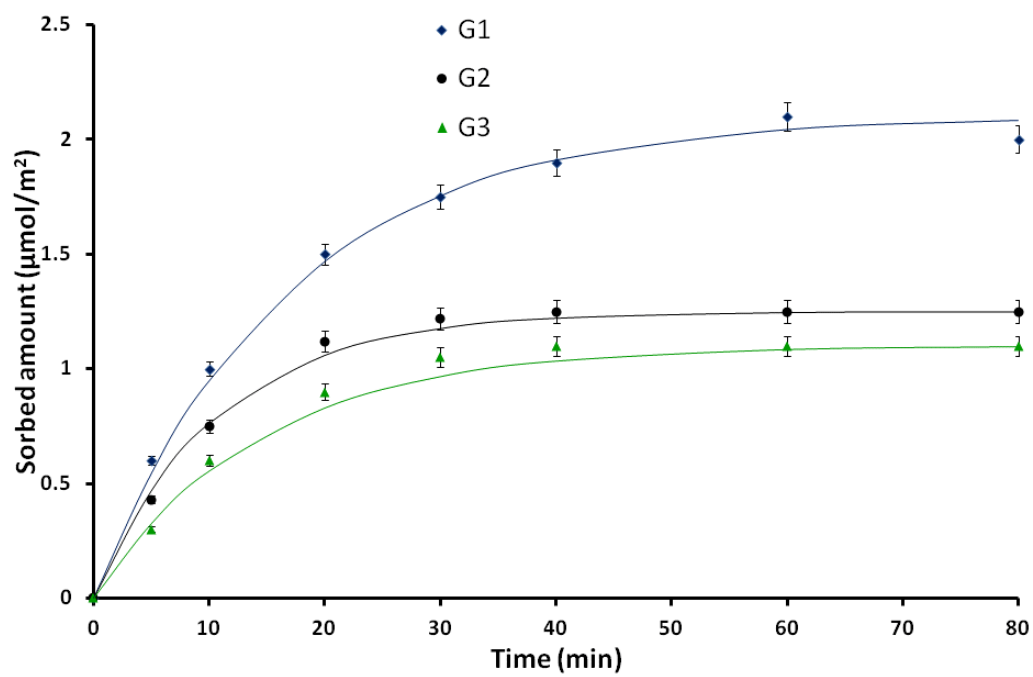
**Figure 1:** (a) Sorption of dissolved  $\text{Fe}^{\text{II}}$  onto three goethites (G1, G2 or G3) vs. time.  $[\text{Fe}^{\text{II}}] = 0.5 \text{ mM}$ ;  $\text{pH} = 6 \pm 0.1$ . Lines represent kinetic model fits. (b) Sorption data onto G1, G2 and G3 vs. pH.  $[\text{Fe}^{\text{II}}] = 0.5 \text{ mM}$ , Lines represent SCM model. Conditions:  $50 \text{ m}^2/\text{L}$  was used as reactive phase concentration,  $T = 20 \pm 1 \text{ }^\circ\text{C}$ ,  $10 \text{ mM NaCl}$  as supporting electrolyte.

**Figure 2:** Experimental breakthrough curves of compound (symbols) and pH (solid line) for three GCS column. Inflowing solution with  $C_0 = 0.5 \text{ mM}$ ,  $\text{pH}_i = 6$ ,  $T = 20 \text{ }^\circ\text{C}$ ,  $10 \text{ mM NaCl}$ . The column was pre-equilibrated with  $10 \text{ mM NaCl}$  for 48 h. Flow rate =  $1 \text{ mL/min}$ .

**Figure 3:** (a) Experimental breakthrough curves of  $\text{Br}^-$  and  $\text{Fe}^{\text{II}}$ . Flow rate =  $1 \text{ mL/min}$ . Experimental data (symbols) and calculated breakthrough curves (PHREEQC-2) using the SCM parameters derived from the batch equilibrium experiments. (b) Experimental breakthrough curves of  $\text{Fe}^{\text{II}}$  at three flow rates in the G1 column ( $0.1$ ,  $0.5$  and  $1 \text{ mL/min}$ ).  $10 \text{ m}^2$  was used as reactive phase amount in each column. Inflowing solution with  $C_0 = 0.5 \text{ mM}$ ,  $\text{pH} = 6 \pm 0.1$ ;  $T = 20 \pm 1 \text{ }^\circ\text{C}$ ,  $10 \text{ mM NaCl}$ ,  $[\text{Br}^-] = 10^{-2} \text{ M}$ .

**Fig.1**

**(a)**



**(b)**

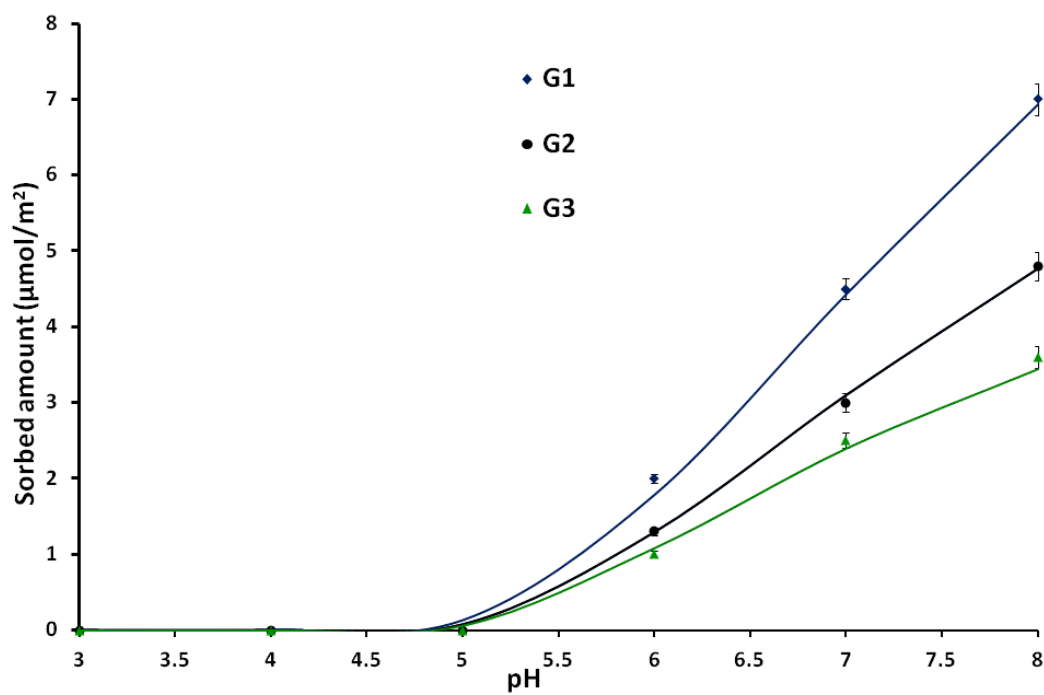




Fig. 2

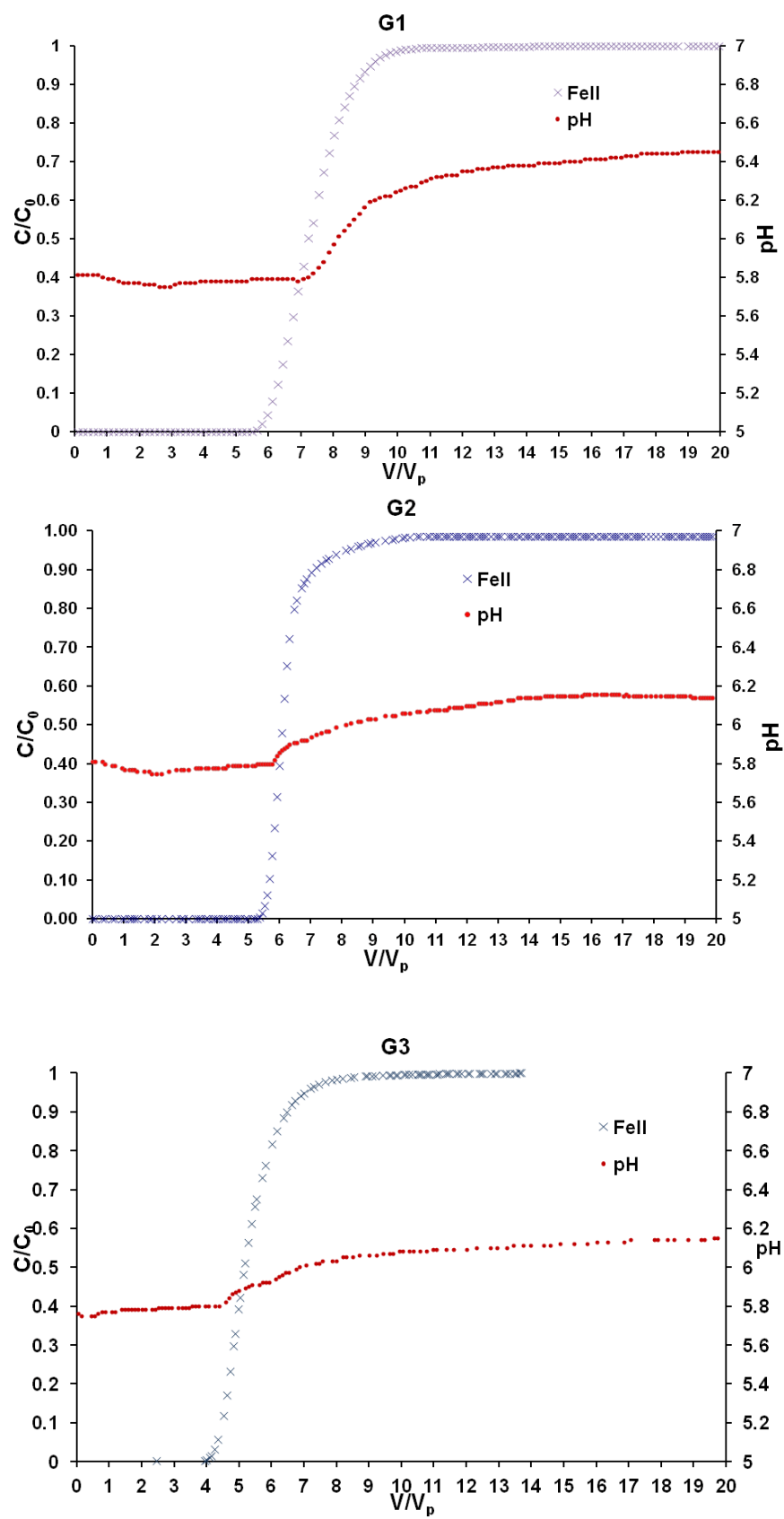
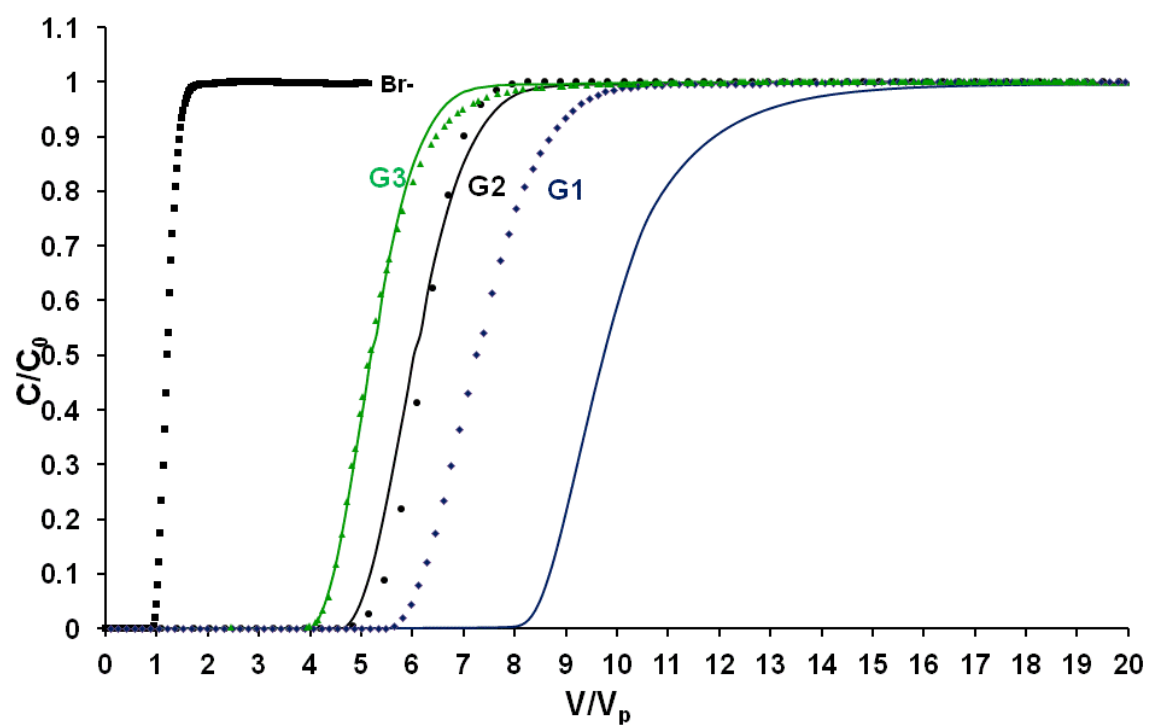


Fig. 3

(a)



(b)

